CHARGED PION PRODUCTION IN e⁺e⁻ ANNIHILATION AT 14, 22 AND 34 GeV CM ENERGY

TASSO Collaboration

R. BRANDELIK, W. BRAUNSCHWEIG, K. GATHER, F.J. KIRSCHFINK, K. LÜBELSMEYER,
H.-U. MARTYN, G. PEISE, J. RIMKUS, H.G. SANDER, D. SCHMITZ, D. TRINES, W. WALLRAFF
I. Physikalisches Institut der RWTH Aachen, Germany [1]

H. BOERNER [2], H.M. FISCHER, H. HARTMANN, E. HILGER, W. HILLEN, G. KNOP, L. KÖPKE,
H. KOLANOSKI, B. LÖHR, R. WEDEMEYER, N. WERMES, M. WOLLSTADT
Physikalisches Institut der Universität Bonn, Germany [1]

H. BURKHARDT, S. COOPER, D. HEYLAND, H. HULTSCHIG, P. JOOS, W. KOCH, P. KOEHLER [3],
U. KÖTZ [4], H. KOWALSKI [4], A. LADAGE, D. LÜKE, H.L. LYNCH [5], P. MÄTTIG, K.H. MESS,
D. NOTZ, J. PYRLIK, D.R. QUARRIE [6], R. RIETHMÜLLER, A. SHAPIRA [7], P. SÖDING, G. WOLF
Deutsches Elektronen-Synchrotron DESY, Hamburg, Germany

R. FOHRMANN, M. HOLDER [8], H.L. KRASEMANN, P. LEU, D. PANDOULAS, G. POELZ, O. RÖMER [9],
R. RÜSCH [10], P. SCHMÜSER, B.H. WIIK
II. Institut für Experimentalphysik der Universität Hamburg, Germany [1]

I. AL-AGIL, R. BEUSELINCK, D.M. BINNIE, A.J. CAMPBELL, P.J. DORNAN, D.A. GARBUTT,
T.D. JONES, W.G. JONES, S.L. LLOYD, J.K. SEDGBEER, R.A. STERN, S. YARKER [11]
Department of Physics, Imperial College, London, England [12]

K.W. BELL, M.G. BOWLER, I.C. BROCK, R.J. CASHMORE, R. CARNEGIE, R. DEVENISH,
P. GROSSMANN, J. ILLINGWORTH, M. OGG [13], G.L. SALMON, J. THOMAS, T.R. WYATT,
C. YOUNGMAN
Department of Nuclear Physics, Oxford University, England [12]

B. FOSTER, J.C. HART, J. HARVEY, J. PROUDFOOT, D.H. SAXON, P.L. WOODWORTH
Rutherford Appleton Laboratory, Chilton, England [12]

E. DUCHOVNI, Y. EISENBERG, U. KARSHON, G. MIKENBERG, D. REVEL, E. RONAT
Weizmann Institute, Rehovot, Israel [14]

and

T. BARKLOW, J. FREEMAN [3], P. LECOMTE [15], T. MEYER [16], G. RUDOLPH, E. WICKLUND,
SAU LAN WU and G. ZOBERNIG
Department of Physics, University of Wisconsin, Madison, WI, USA [17]

The inclusive production of $\pi^{\pm}$ mesons in e^+e^- annihilation has been measured at c.m. energies of 14, 22 and 34 GeV for pion momenta between 0.3 and 10 GeV/c. The fraction of pions among the charged hadrons is above 90% at 0.4 GeV/c and decreases to about 50% at high momenta. The scaled cross sections (s/β) $d\sigma/dx$ at 14, 22 and 34 GeV as well as the 5.2 GeV data from DASP have a rather similar x dependence. After integration over the x range from 0.2 to 0.6 the cross sections indicate a monotonic decrease with increasing centre-of-mass energy.

The inclusive production of hadrons in e^+e^- annihilation is of considerable interest as a test of scale invariance and of different fragmentation models. In comparison with data on neutral particle production [1–3], measurements of identified charged particle spectra in the PETRA energy range [4] have so far been restricted to significantly lower values of the fractional hadron energy $x = 2E_{hadron}/W$, where W is the centre of mass energy. In the present paper we report on measurements of charged pion production covering a wide range in x at energies W = 14, 22, and 30 to 37 GeV ($\overline{W}$ = 34 GeV).

The experiment was performed with the TASSO detector at PETRA. The momentum of charged particles was measured in the central detector [5] with an accuracy $\sigma_p/p = 0.017 (1 + p^2)^{1/2}$ (p in GeV/c). Pions were separated from kaons and protons by means of time-of-flight (TOF) for momenta between 0.3 and 1.5 GeV/c and by threshold Čerenkov counters for momenta between 0.8 and 10 GeV/c. The TOF separation was done with the inner and the hadron arm time-of-flight counter systems (ITOF and HATOF, respectively).

The ITOF system is located between the central tracking chambers and the magnet coil at a radial distance of 132 cm from the beam axis. It consists of 48 counters with phototubes at both ends and covers a solid angle of 82% of 4π. A resolution of $\sigma = 0.38$ ns was achieved averaged over tracks in hadronic e^+e^- annihilation events. ITOF measurements were used to determine the pion yields for momenta between 0.3 and 1.0 GeV/c.

The HATOF as well as the Čerenkov counters are mounted outside the 10 cm thick aluminium magnet coil in the TASSO "hadron arms". Each hadron arm consists of the following components:

– a planar drift chamber with one layer of horizontal signal wires and vertical cathode strips;

– three types of threshold Čerenkov counters, arranged sequentially, using as radiators silica aerogel ($n = 1.024 \pm 0.002$), freon 114 ($n = 1.0014$) and CO_2 ($n = 1.00043$);

– the array of 48 HATOF counters, with phototubes at both ends;

– lead-scintillator shower counters, 7.4 radiation lengths thick;

– 87 cm of iron absorber and a 4 layer tube chamber for muon detection.

A full description of the HATOF counters has already been published [6]. Briefly, they are located 5.5 m from the interaction point and cover a solid angle of 20% of 4π. The resolution is $\sigma = 0.45$ ns, allowing π, K, and p separation in the momentum interval from 0.5 to 1.5 GeV/c.

A detailed technical account of the Čerenkov counter system can be found elsewhere [7]. Here we restrict ourselves to a brief outline of the system and concentrate mainly on its particle identification properties.

The counters cover polar angles θ, measured with respect to the beam axis, from 50° to 130° and azi-

muthal angles ϕ, measured with respect to the horizontal plane, from $-26°$ to $+26°$ and from $154°$ to $206°$. The total solid angle subtended is 19% of 4π. The threshold momenta for pions in the three counters are 0.6, 2.7, and 4.8 GeV/c, respectively. The corresponding numbers for kaons are 2.2, 9.4, and 16.9 GeV/c and for protons 4.2, 17.8, and 32 GeV/c. In the present analysis only the aerogel and freon counters were used to identify pions.

The Čerenkov counters are mechanically subdivided into 16 cells per arm each covering a $\Delta\theta$ of $10°$ and a $\Delta\phi$ of $26°$. The gas counters are subdivided further into half cells with a $\Delta\phi$ of $13°$ by two elliptical mirrors focusing the light onto different phototubes. In the aerogel counters light collection via mirrors is difficult due to the diffuse light scattering in the radiator itself. Instead each cell is lined with highly reflective white Millipore paper and viewed by six photomultipliers (ref. [7]).

The performance of the Čerenkov counters was studied in prototype measurements in a hadron test beam. The counters have been constantly monitored by analyzing cosmic ray muons recorded concurrently with the e^+e^- data. For the aerogel counters we have determined an efficiency of 95% averaged over all Čerenkov cells and the whole data taking period. The gas counters have efficiencies well above 99% for high-momentum muons. Their refractive indices have been measured periodically and have been found to be constant to within 3×10^{-5}.

Hadronic final states from e^+e^- annihilation were selected using the charged particle information from the central detector and applying the same cuts as in ref. [8]. In the TOF analyses we verified by Monte Carlo calculations, using the same model [9,10] as in our previous analyses [1,11], that the track acceptance cuts (in particular the demand that only one particle enters a particular TOF counter) do not introduce any bias for a given particle species. The relative yields of pions, kaons, and protons in each momentum interval were determined by comparing the measured mass-squared distribution with those expected for different particle types. The latter, as well as the acceptances for individual particle species, were derived by tracking Monte Carlo simulated events through the detector. The results were corrected for decay losses, nuclear interactions and absorption in the material in front of the counters, and for the contamination due to elec-

trons from converted photons. Prompt leptons were subtracted using the Monte Carlo model.

The sample of charged tracks inside the Čerenkov counter acceptance with momenta above 0.8 GeV/c consists of 1319 tracks at $W = 14$ GeV, 1423 at $W = 22$ GeV, and 4360 at $\bar{W} = 34$ GeV. To ensure unambiguous particle identification a central detector track has to satisfy the following criteria: (1) It has to penetrate the coil material without inelastic nuclear interaction; (2) the track should not be accompanied by another charged track or (3) by a shower in the same Čerenkov cell. These requirements will be discussed below.

(1) Penetration of the coil: Before entering the Čerenkov counters the particles have to traverse a material thickness of 31 g/cm^2 of mainly aluminum. It is essential to recognize inelastic nuclear interactions, since an absorbed pion may be considered as a particle without light in the appropriate Čerenkov counters, i.e. as a kaon or proton. The planar drift chamber mounted directly behind the coil is used for this purpose. A central detector track is considered to have passed through the coil without nuclear interaction if the planar drift chamber has a hit within an "acceptance window" covering about 3 times the average multiple scattering angle. The percentage of accepted tracks amounts to 60% at 0.8 GeV/c and rises to 80% above 3 GeV/c. The data agree with the transmission probability of the coil material as computed from nuclear cross sections.

(2) Discrimination against overlapping tracks: The Čerenkov information of an accepted track may be altered by other nearby tracks. The track in question is discarded if a second track with a momentum above the pion threshold in aerogel enters the same Čerenkov cell. The fraction of tracks surviving this "two-track" cut amounts to 95% for the hadronic events at $W = 14$ GeV and to 85% for the data at 34 GeV which have much larger multiplicity and stronger jet collimation.

(3) Discrimination against showers: Showers produced by photon conversion in the coil are mainly recognized by large pulse heights in the aerogel counters. The pulse height distribution obtained for single fast muons is Poisson-like with an average value corresponding to 3 photoelectrons. Showering particles on the other hand, produce a rather wide distribution extending up to 50 photoelectrons for 7 GeV/c electrons. Requiring a pulse height of less than six photo-
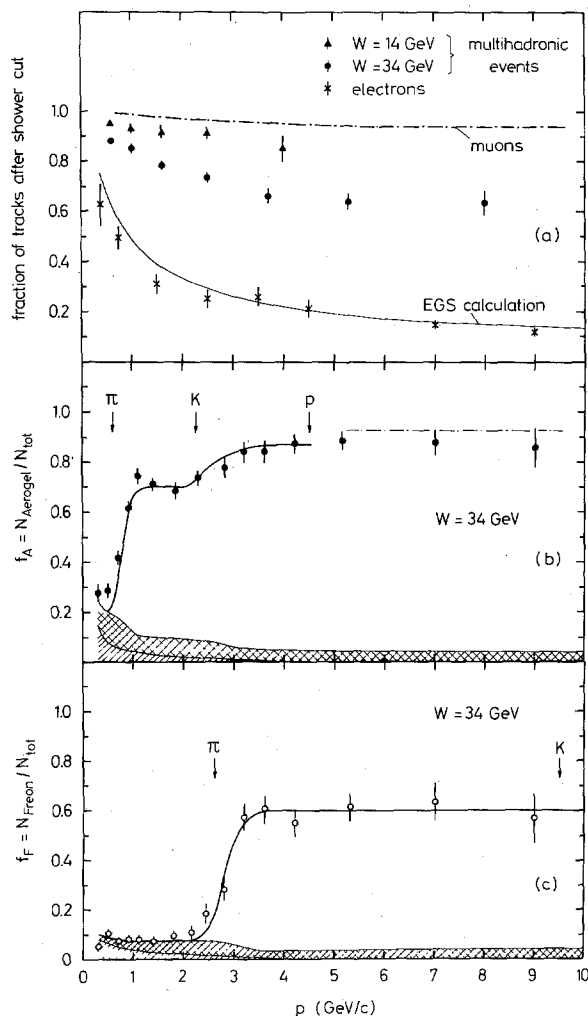
Fig. 1. (a) Fraction of tracks from multihadron events at W = 14 and 34 GeV with less than six photoelectrons in the aerogel. The effect of this cut on electrons from one- and two-photon events is also shown and compared to the EGS calculation (solid line; see text). The dashed—dotted line shows the fraction of cosmic ray muons accepted by the cut. (b) Fraction of accepted tracks from multihadron events at $\overline{W}$ = 34 GeV, which produce light in aerogel. The arrows indicate the pion, kaon and proton Čerenkov thresholds. The solid line is the calculated pion and kaon threshold curve assuming constant particle ratios. The dashed area represents the electron contribution and the cross-hatched area the accidental background (see text). The dashed—dotted line shows the efficiency plateau in aerogel after application of the six photoelectron cut. (c) Fraction of accepted tracks which produce light in freon. Background as in (b).

electrons leaves 94 to 98% of the cosmic muons but removes a large fraction of the showers. The effect of this cut has been studied quantitatively by analyzing Bhabha scattering and e^+e^- pair production by two-photon collisions. The fraction of electrons passing the cut is plotted in fig. 1a as a function of momentum. The data agree quite well with a Monte Carlo computation based on the electromagnetic shower program EGS [12]. Also plotted in fig. 1a is the fraction of multihadronic event tracks from the sample accepted by criteria (1) and (2) that survive the six photoelectron cut. Here the losses are larger than for muons because of showers leaking into the same aerogel counter. The losses increase with momentum since high-momentum tracks are on the average closer to the jet axes of the events than low-momentum tracks. An additional shower cut designed to remove high-energy electrons was applied by requiring an energy of less than 2 GeV in the hadron arm shower counters. Minimum ionizing particles deposit a shower equivalent of about 200 MeV with a tail out to 600 MeV.

The fraction of tracks inside the Čerenkov counter acceptance which remain for particle identification is given by the product of the probabilities to penetrate the coil and to pass the two-track and shower cuts. This fraction amounts to $(50 \pm 1.5)\%$ at $W = 14$ GeV and drops with increasing c.m. energy to $(47 \pm 1.5)\%$ at 22 GeV and $(40 \pm 1)\%$ at 34 GeV. Above 1 GeV/c it depends only slightly on the momentum, so that the accepted hadron arm tracks have almost the same momentum and transverse momentum spectra as the central detector tracks. In addition, we verified that criteria (1), (2), and (3) do not introduce a bias in the event selection. The events accepted for the Čerenkov analysis have the same distributions in multiplicity and sphericity as the central detector events.

For the data sample surviving the previous cuts, the rates in the various Čerenkov counters have been studied as a function of momentum. This is demonstrated for the data at $\overline{W} = 34$ GeV which have the highest statistics. In fig. 1b we plot the normalized aerogel counter rate $f_A = N_{aerogel}/N_{tot}$, i.e. the number of particles in a given momentum interval which produce light in aerogel, divided by the total number of particles in that interval. A steep rise is observed above 0.6 GeV/c, showing the pion threshold in aerogel. This is followed by a plateau between 1 and 2.2 GeV/c and then a second rise is seen above the

kaon threshold in aerogel. The statistics are not sufficient to observe the proton threshold. The normalized rate of the freon Čerenkov counters $f_F = N_{freon}/N_{tot}$ is shown in fig. 1c as a function of momentum. The pion threshold between 2.7 and 3 GeV/c is clearly seen. Both Čerenkov counters have a nonvanishing rate below the pion (and muon) threshold. In the case of the freon counters we obtain $f_F = (8.2 \pm 0.6)$% at $\bar{W}$ = 34 GeV and $f_F = (4.5 \pm 0.7)$% at W = 14 GeV for momenta between 0.3 and 2 GeV/c. A large fraction of this rate is due to electrons which are mainly produced by photon conversion in the beam pipe. The electron contribution to the aerogel and the freon counter rate is shown as a dashed area in figs. 1b, c. It was estimated from a Monte Carlo simulation of $e^+e^- \to q\bar{q}, q\bar{q}g$ [9,10]. In this simulation electrons were traced through the coil with the EGS program and were required to pass the acceptance, two-track and shower cuts.

The remaining part of the Čerenkov rate below the pion threshold can be accounted for by non-recognized showers coinciding with hadrons and producing the Čerenkov signal. The probability of such coincidences was determined from the data itself. For this purpose we investigated Čerenkov cells which were not hit by central detector tracks. The probability to observe light in such an "empty" Čerenkov cell was found to be 10–25% for aerogel and 5–10% for freon, depending on the distance to the jet axis. (These numbers refer to the data at $\bar{W}$ = 34 GeV; they are smaller at 14 GeV). By multiplying these probabilities with the fraction of hadrons which do not produce light in the Čerenkov counters, we obtained the background indicated as a cross-hatched area in figs. 1b, c.

The pion yield was computed from the Čerenkov rates with the background properly subtracted. For momenta between 0.8 and 2.6 GeV/c the aerogel counters in anticoincidence with the freon counters were used to define pions. The veto signal from the gas counters reduced the background plotted in fig. 1b by almost a factor of three, leading to a negligible electron contamination of the pion sample. (Between 2.3 and 2.6 GeV/c a small correction was applied for kaons whose average efficiency in aerogel is about 30% in this interval). The pion threshold region in freon from 2.6 to 3 GeV/c was omitted from the analysis. Above 3 GeV/c the pion yield was obtained from the freon counter rate after subtraction of the

background shown in fig. 1c. Again the electron contamination is negligible because of the very small probability to observe high-momentum electrons with less than six photoelectrons in aerogel and less than 2 GeV in the shower counters.

In order to determine the pion fraction $f_\pi = N_{\pi\pm}/N_{h\pm}$, where $N_{h\pm}$ is the number of charged hadrons, the Čerenkov data were corrected for the difference in nuclear absorption of pions, kaons, and protons/antiprotons in the material between the event vertex and the Čerenkov system and for decay of pions and kaons. The pion fraction is reduced by only 0.02 to 0.04. Prompt muons were subtracted reducing f_π by less than 0.01.

Within statistical errors equal numbers of positive and negative pions have been observed at all momenta and c.m. energies. In the regions of overlap, the pion fractions as determined by the ITOF, HATOF, and Čerenkov analyses are in good agreement and have been combined weighting each result by its error. The pion fractions are plotted in fig. 2 against the particle momentum. They are above 90% at 0.4 GeV/c and drop to about 50% at high momenta. Charged pions from K_s^0 decays have not been subtracted. It is interesting to note that for momenta below 1 GeV/c the pion fractions are independent of W when plotted against p rather than against the scaled momentum $x_p = p/p_{beam}$.

The cross sections for the inclusive production of charged hadrons, $e^+e^- \to h^\pm X$, have been derived from the central detector data. The procedure will be
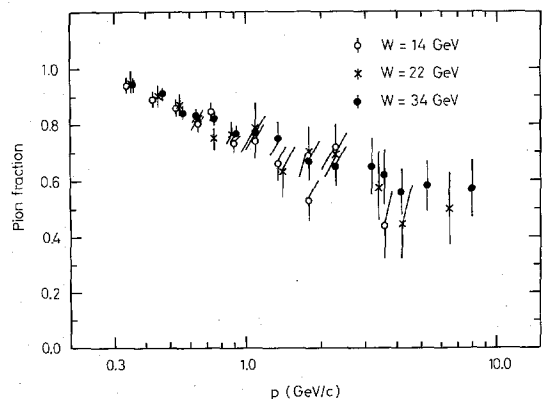

Fig. 2. The pion fractions $f_\pi = N_{\pi\pm}/N_{h\pm}$ as a function of the particle momentum p for $\bar{W}$ = 14, 22 and 34 GeV. The K_s^0 decay contribution to the pion yield is included.
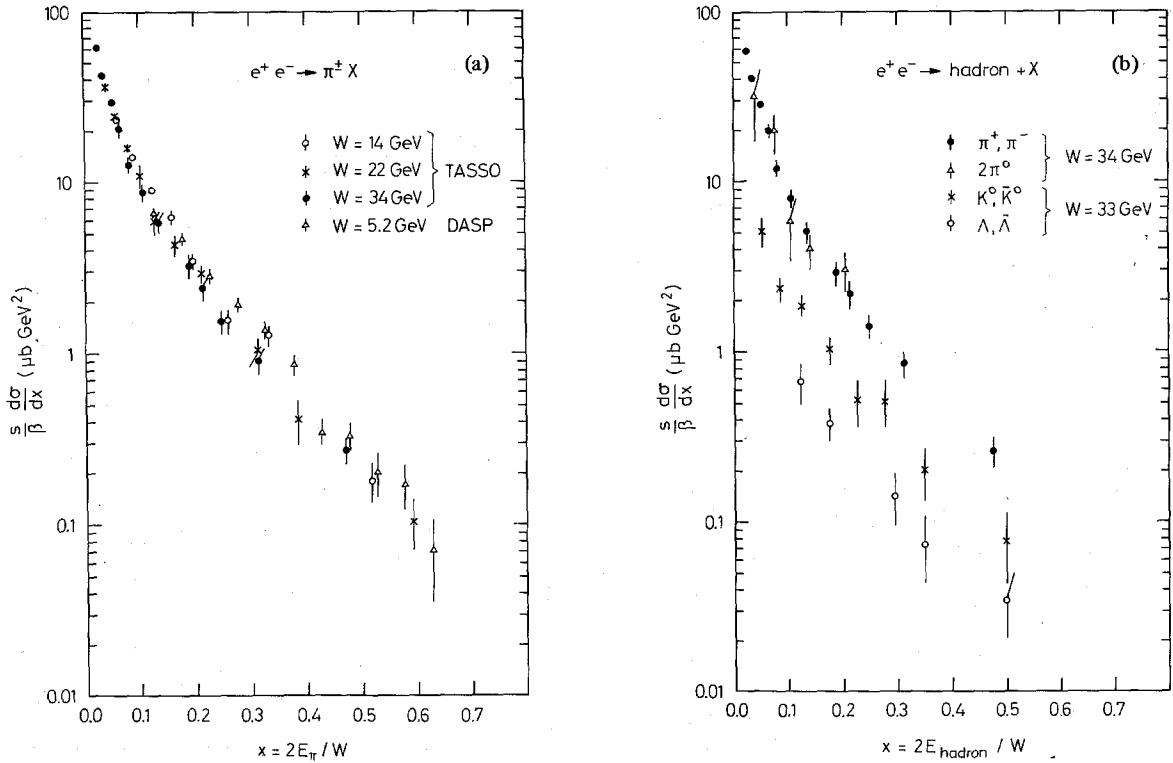
Fig. 3. (a) The scaled cross sections $(s/\beta)d\sigma/dx$ for $e^+e^- \to \pi^\pm X$ at W = 14, 22, and 34 GeV including the contribution from K_S^0 decays. Also shown are the DASP data at W = 5.2 GeV. (b) The scaled cross sections for $e^+e^- \to$ hadron + X at W = 33–34 GeV shown for $\pi^\pm$ (this experiment), π^0 (ref. [1]), K^0, $\overline{K}^0$ and Λ, $\overline{\Lambda}$ (ref. [2]). The K_S^0 decay contribution to the $\pi^\pm$ and π^0 yield has been subtracted.

described in a separate publication. We have computed the cross sections for charged-pion production by multiplying these values with the pion fractions. In fig. 3a we show the scaled cross sections $(s/\beta)d\sigma/dx$ for $e^+e^- \to \pi^\pm X$ ($s = W^2$ and $\beta = p_\pi/E_\pi$). The error bars include all statistical and systematic errors except for an overall normalization of 5.5% at W = 34 GeV, 6.3% at W = 22 GeV, and 8.5% at W = 14 GeV. The scaled cross sections agree quite well with our earlier results on $\pi^\pm$ production at W = 12 and 30 GeV which had lower statistics and were restricted to a narrower x range ($x \lesssim 0.2$ at 12 GeV and $x \lesssim 0.08$ at 30 GeV). The scaled cross sections obtained in the present experiment do not exhibit a significant energy variation between 14 and 34 GeV but they are somewhat lower than the 5.2 GeV data [+1] from

[+1] We compare with DASP data at W = 5.2 GeV and not with those at $W \leqslant 5.0$ GeV because the latter might be enhanced by effects from the charm threshold region (see ref. [13]).

DASP [13] which are also shown in fig. 3b. For a quantitative comparison we have integrated $(s/\beta)d\sigma/dx$ over the range $0.2 \leqslant x \leqslant 0.6$ and have obtained the following values for the integral $\tilde{\sigma}(W)$:

$\tilde{\sigma}(5.2) = 0.396 \pm 0.063 \ \mu b \ GeV^2$,

$\tilde{\sigma}(14) = 0.336 \pm 0.041 \ \mu b \ GeV^2$,

$\tilde{\sigma}(22) = 0.292 \pm 0.038 \ \mu b \ GeV^2$,

$\tilde{\sigma}(34) = 0.270 \pm 0.031 \ \mu b \ GeV^2$.

The errors include all statistical and systematic errors of the present experiment and the 15% normalization uncertainty of the DASP data. The integrated cross sections suggest a monotonic decrease as a function of W, corresponding to a scaling violation effect with a significance of two standard deviations.

In fig. 3b we compare the 34 GeV $\pi^\pm$ data with our published π^0 data [1] at $\overline{W}$ = 34 GeV and K^0 and Λ data [2] at $\overline{W}$ = 33 GeV; the contribution from K_S^0

decays has been subtracted for both $\pi^\pm$ and π^0. The scaled cross sections have a rather similar x dependence. Moreover, the π^0 data, multiplied by a factor of two, are in good agreement with the $\pi^\pm$ results. Integrated over the momentum range from 1 to 4 GeV/c the ratio between neutral- and charged-pion production is found to be $2\sigma(\pi^0)/[\sigma(\pi^+) + \sigma(\pi^-)]$ = 1.01 ± 0.20. For the data at W = 14 GeV, the value obtained for this ratio is 0.79 ± 0.17 [*2].

We wish to thank all persons at DESY and at the University of Hamburg, who contributed to the design, construction, and testing of the Čerenkov counters. We are particularly indebted to U. Balszuweit for producing the aerogel, to G. Krohn for assembling the Čerenkov counters and to C.H. Sellmer for aluminizing the mirrors. We gratefully acknowledge the tremendous efforts of the PETRA machine group for the sustained high luminosity running. Those of us abroad wish to thank the DESY directorate for the hospitality extended to us while working at DESY.

[*2] The π^0 cross sections at W = 14 GeV were evaluated in ref. [1] assuming the value of 3.9 ± 0.4 for $R = \sigma(e^+e^- \rightarrow \text{hadrons})/\sigma(e^+e^- \rightarrow \mu^+\mu^-)$. A more detailed analysis gave $R = 4.14 \pm 0.30$, which is the value used here.

References

[1] TASSO Collab., R. Brandelik et al., Phys. Lett. 108B (1982) 71.
[2] TASSO Collab., R. Brandelik et al., Phys. Lett. 105B (1981) 75; 94B (1980) 91.
[3] JADE Collab., W. Bartel et al., Phys. Lett. 104B (1981) 325;
PLUTO Collab., Ch. Berger et al., Phys. Lett. 104B (1981) 79.
[4] TASSO Collab., R. Brandelik et al., Phys. Lett. 94B (1980) 444.
[5] TASSO Collab., R. Brandelik et al., Phys. Lett. 83B (1979) 261;
H. Boerner et al., Nucl. Instrum. Methods 176 (1980) 151.
[6] K.W. Bell et al., Nucl. Instrum. Methods 179 (1981) 27.
[7] H. Burkhardt et al., Nucl. Instrum. Methods 184 (1981) 319;
G. Poelz and R. Riethmüller, DESY report 81/055;
Nucl. Instrum. Methods, to be published.
[8] TASSO Collab., R. Brandelik et al., Z. Phys. C4 (1980) 87.
[9] P. Hoyer et al., Nucl. Phys. B161 (1979) 349.
[10] T. Meyer, DESY report 81/46 (1981).
[11] TASSO Collab., R. Brandelik et al., Phys. Lett. 94B (1980) 437.
[12] R.L. Ford and W.R. Nelson, SLAC report 210 (1978).
[13] DASP Collab., R. Brandelik et al., Nucl. Phys. B148 (1979) 189.